RSC Advances

This is an *Accepted Manuscript*, which has been through the Royal Society of Chemistry peer review process and has been accepted for publication.

Accepted Manuscripts are published online shortly after acceptance, before technical editing, formatting and proof reading. Using this free service, authors can make their results available to the community, in citable form, before we publish the edited article. This *Accepted Manuscript* will be replaced by the edited, formatted and paginated article as soon as this is available.

You can find more information about *Accepted Manuscripts* in the Information for Authors.

Please note that technical editing may introduce minor changes to the text and/or graphics, which may alter content. The journal's standard Terms & Conditions and the Ethical guidelines still apply. In no event shall the Royal Society of Chemistry be held responsible for any errors or omissions in this *Accepted Manuscript* or any consequences arising from the use of any information it contains.

ROYAL SOCIETY OF CHEMISTRY

www.rsc.org/advances

RSC Advances

RSC Advances

Dynamic Article Links ►

Cite this: DOI: 10.1039/c0xx00000x

www.rsc.org/xxxxxx

paper

One step preparation of porous polyurea by reaction of toluene diisocyanate with water and its characterization

Hui Han[a], Shusheng Li[a,b], Xiaoli Zhu[a], Xubao Jiang[a] and Xiang Zheng Kong*[a]

Received (in XXX, XXX) Xth XXXXXXXXX 20XX, Accepted Xth XXXXXXXXX 20XX

DOI: 10.1039/b000000x

Porous polyurea (PPU) is prepared through a simple protocol by reacting toluene diisocyanate (TDI) with water in binary solvent of water-acetone, and the process is optimized. Porosimetric test demonstrates that PPU possesses typical properties of porous materials. The structure of the material is characterized by Fourier transform infrared (FTIR), NMR (^{1}H & ^{13}C) and X-ray diffraction (XRD). FTIR analysis shows that TDI is full reacted. Microstructure analysis of PPU by NMR reveals that PPU is consisting of short polyurea chains with degree of polymerization about 15. The presence of crystallinity in PPU is confirmed by XRD, which shows three diffraction peaks, for which the corresponding chain conformations, based on interplanar spaces owing to different hydrogen-bonding, are depicted. TGA analysis demonstrates that PPU is of high thermal stability, and no degradation is seen before 270 °C. DSC test reveals that no obvious glass transition is observed owing to intensive hydrogen-bonding.

Introduction

Polyureas (PU) can be synthesized either through condensation polymerization of multifunctional isocyanates (NCO, commonly diisocyanate or triisocyanate) with polyamines, or through the reaction of multifunctional isocyanate in excess with water with release of carbon dioxide, which turns the isocyanate groups to amines, followed by the same condensation polymerization of the isocyanate with the in-situ produced amines.[1-3] PU has been well known to be of thermal shock and abrasion resistance, high impact resistance, good flexibility and water repellency as well as fast cure etc.[4] Common applications are protective coating materials for different structural materials, including concrete[5-6] and metals,[7-9] for instance. Up to date, PU materials have been commercialized in a variety of fields, and relevant researches are being conducted to explore their novel applications.[2,3,10-14]

Up to now, most of the reported studies on PU syntheses and structure analyses were mainly focused on the condensation polymerization using diisocyanate and diamines,[15-18] fewer using multifunctional amines or isocyanates.[19,20] It is to stress that the pathway to PU synthesis, via multi-functional isocyanate reaction with water, followed by condensation reactions between the same isocyanates and the in-situ formed amines,[1-3,21-22] is advantageous because the reactions involve only isocyanate monomer without need of any other chemicals, and in general, it can be easily performed at ambient temperature. Nevertheless, little effort has been done on these PU's in comparison with those from copolymerization of isocyanates with amines. The reaction to produce PU by reacting isocyanate with water has been predominantly used for environmental curing of films baring NCO groups or for foaming polyurethanes.[21] Among the numbered studies, there were reports on the preparation of highly uniform microspheres by reacting isophorone diisocyanate with water in a binary solvent mixture of water-acetone,[1,2] and that on porous PU aerogels through reactions of Desmodur diisocyanate and triisocyanate with water in the presence of a catalyst.[21]

Another relevant topic to this work is porous material, which is well studied and widely applied in different industries. Porous materials may be inorganic materials,[23] polymers[24-26] or their combinations.[27,28] Because of the easy control of their specific surface area, their designable pore structure and functionalization, porous polymers have been gaining more importance and widely applied to different fields including conventional applications as ion-exchange,[24,29] adsorption,[24,30] chromatography[31,32] and catalysis,[33,34] for instances, and new emerging applications such as biological technology and tissue engineering,[35,36] microreactor,[28] sensor technology etc.[37-39] Commonly used processes for the preparation of porous polymer materials include suspension polymerization, high internal phase emulsions[25] or dispersion polymerization[24,25,40] and a variety of emulsion polymerization etc.[24,41,42] All these processes are commonly labelled as heterogeneous polymerization, where surfactants and stabilizers are compulsory to ensure the stability of the polymerization and the formation of the desired porous structures in the products. In addition, the porous materials thus obtained usually have to go through a chemical modification, prior to their practical application, in order to endow them with functional groups, such as amine, sulfonate, hydroxyl, carboxyl, imine, thiol and amidoxime etc.[43-48] This demonstrates that, to fabricate a functional porous polymer material, multiple steps are usually required, each step is more or less sophisticated with long-lasting and high energy consuming, and the chemical modification leads often to adverse effects on the performance of the porous materials.[48] Furthermore, the organic porogens, surfactants and

RSC Advances Accepted Manuscript

stabilizers commonly used in these processes, hard to be full removed, are unpleasant, particularly in biological and medical applications.

In this paper, porous polyurea (PPU) with functional amine groups was easily prepared via a simple one-step precipitation polymerization in H_2O-acetone binary solvent, using toluene diisocyanate (TDI) as the only monomer, in which neither any additives as porogen, surfactant or stabilizer were used, and nor any chemical modification on the resultant porous polymer was needed. Characterization of the materials demonstrated that PPU thus prepared possessed high surface area and pore volume. As afore mentioned, very limited studies on PU syntheses via isocyanate reaction with water, works on their structure characterizations are also rarely available. The microstructure of this PPU is also characterized using different instrumentation including nuclear magnetic resonance (NMR, ^{1}H and ^{13}C), X-ray Diffraction (XRD), Fourier transform infrared spectroscopy (FTIR). Thermal properties of this PPU were also tested.

Experimental

Materials

Toluene diisocyanate (TDI 8020, industrial grade, with 80% of 2,4- and 20% of 2,6-TDI according to the supplier, Wanhua Chemicals, China), acetone (AR, Tianjin Damao Chemicals), potassium bromide (KBr, AR, Tianjin Kemiou Chemical Reagent Co.) and 2,4-diaminotoluene (TDA, CP, Aladdin) were used as received. Dimethyl sulfoxide-d6 (DMSO-d_6, 99.9% atom D) and deuterium oxide (D_2O, 99.9% atom D), both used in NMR tests, were purchased from Aladdin. Water used throughout this work, except in NMR test, was double-distilled.

PPU synthesis

To a round bottom flask of 120 mL capacity, 90.0 g of H_2O-acetone mixture at mass ratio of 3/7 was first charged. The flask was immersed in a water bath at 30 °C, and 10.0 g of TDI was added at a rate of 20 mL·h^{-1} under stirring at 300 r·min^{-1}. The polymerization was allowed to continue for 2 h after TDI addition completed, followed by centrifugation to separate the solid, which was rinsed twice by acetone and dried at 70 °C under vacuum to get a powder polymer product. In order to optimize the process, polymerizations were also carried out at different polymerization temperature and with varied TDI feeding rate.

Characterization and instrumentation

PPU morphology was observed under scanning electron microscope (SEM, FEI Quanta 200). Its porous properties were determined by Hg intrusion using Micromeritics porosimeter (AutoPore IV 9500). Pore size below 100 nm and the size distribution were also analyzed by N_2 adsorption-desorption using a surface area analyzer (BET, Quantachrome, Nora 200E). Fourier transform infrared spectroscopy (FTIR) analysis of PPU was done from 400 cm^{-1} to 4000 cm^{-1} on a Brüker spectrometer (Vertex 70) with the sample compressed in KBr pellet. For NMR analysis of high-resolution, PPU was dissolved in DMSO-d_6 and the tests carried out with a Brüker instrument (Advance III) at 400 MHz for ^{1}H and 100 MHz for ^{13}C. Spectra were obtained with a 5-mm-QNP probe at 298 K. Tetramethylsilane was used as the internal reference. To understand the crystallization and structure of the sample, powder X-ray diffraction (XRD) was recorded on a diffractometer (Brüker D8 Focus) in the two-theta range from 6° to 60° using a Cu-K radiation source. Differential scanning calorimetry (DSC) test was conducted, from 30 °C to 450 °C at a heating rate of 5 °C/min, using a Mettler-Toledo instrument (DSC 822) in a nitrogen atmosphere. Differential thermal analysis (DTA) and thermogravimetric analysis (TGA) were carried out using Perkin-Elmer equipment (Pyris Diamond TG/DTA) with the temperature range scanned from 30 °C to 500 °C at a heating rate of 10 °C/min in a nitrogen atmosphere.

Results and discussion

Polyurea synthesis by reacting TDI with water and its characterization

With TDI added to the binary solvent of H_2O-acetone, water was playing a dual role as a reactant and a component in the binary solvent. As reactant, it reacts with isocyanate group (NCO) on TDI molecules to yield CO_2 and amine. The amine molecules generated continue to react with NCO to form linear polyurea, as illustrated in Scheme 1. In principle, biuret formation by NCO reacting with hydrogen of carbamido to form crosslinked PU will not occur because specific conditions (high temperature, catalyst) are required for this reaction.[49,50] As a component in the solvent, the presence of water is compulsory to promote the precipitation of the oligomers and making the polymerization to be a precipitation polymerization. The yield of the product was 100% thanks to the step polymerization mechanism involved as schematized in Scheme 1. Fig. 1 shows SEM images of the as-prepared PPU. It is seen that the material is of irregular granular form. The size of the granules varies from 10 μm to 20 μm. Porous structure was visible on the surface of the granules. Under SEM of high magnification, micron-sized pores are clearly seen (Fig. 1B).

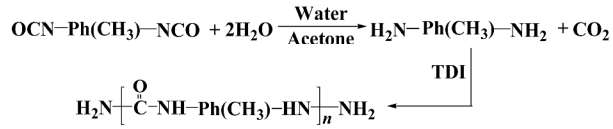

Scheme 1 Presentation of polyurea formation through precipitation polymerization of TDI with water

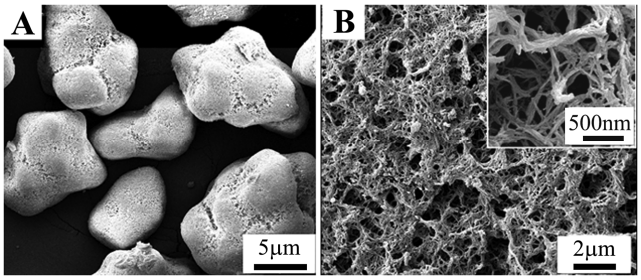

Fig. 1 SEM images of PPU prepared by reacting TDI with water followed by precipitation polymerization in water-acetone

Pore volume and pore size distribution curves from intrusive mercury test are given in Fig. 2. At start of the test at low pressure, larger pores were first filled with Hg, followed gradually by Hg intrusion in the pores of smaller size with pressure increase. Fig. 2 demonstrates that the integrated pore volume (integrated) was in constant increase in the full range of

RSC Advances Accepted Manuscript

This journal is © The Royal Society of Chemistry [year]

the pore size tested (2 nm to 130 μm), indicating the presence of the pores with continuous size variation in the tested span, and the largest contribution to pore volume was by large pores with size varying from 10 μm to 40 μm, followed by those from 3 nm to 100 nm. From Fig. 2, the specific surface area was of 161.68 $m^2 \cdot g^{-1}$, the pore volume of 2.20 $cm^3 \cdot g^{-1}$ with the porosity of 71.77%. For the pores below 100 nm, BET test was carried out, which gave the specific surface area of 157.4 $m^2 \cdot g^{-1}$ and pore volume of 0.38 $cm^3 \cdot g^{-1}$. Comparing these data, it is obvious that the specific surface area was mainly contributed by small pores of size below 100 nm, and pore volume mainly by large pores of size above 100 nm. All these demonstrate that this material is a typical porous material.[51-53]

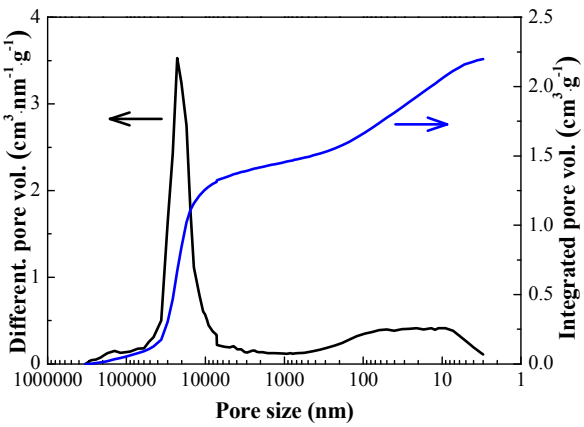

Fig. 2 Pore size distribution and integrated pore volume of PPU

TDI concentration and porous property of PPU

Since TDI was added into the reactor at a constant rate (20 $mL \cdot h^{-1}$) in all runs, it is easy to conceive that TDI concentration was in constant increase with polymerization time in a similar way for runs with different TDI concentration, which means that, a given polymerization with a higher TDI concentration comprehends all the runs with TDI concentrations lower than this given run if it is stopped at an appropriate time. For instance, for the run with 10 wt% TDI (where 10 g or 8.20 mL of TDI was added in about 25 min at constant rate of 20 $mL \cdot h^{-1}$), when a quarter of TDI was added, the polymerization process and the profile of TDI concentration variation was quite the same as that of 2.5 wt% at end of the polymerization; and for the same run with 10 wt% of TDI with half of TDI added, the polymerization was the same as that of 5.0 wt%. This is determined by the nature of the protocol where TDI was added at a constant rate for all runs. With this in mind, polymerizations with varied feeding rate of TDI were carried out to study the influence of TDI concentration on the polymerization and the properties of the porous material. In this case, TDI concentration for a given run at any given polymerization time was different from another one with different TDI feeding rate. Porous properties of PPU prepared with TDI feeding rate varied from 10 $mL \cdot h^{-1}$ to 30 $mL \cdot h^{-1}$ and that with one single shot were measured, the results listed in Table 1.

The data in Table 1 indicate that PPU prepared with lower TDI feeding rate (10 & 20 $mL \cdot h^{-1}$) is characterized by higher specific surface area (>160 $m^2 \cdot g^{-1}$), larger pore volume (>2.1 $cm^3 \cdot g^{-1}$) and higher porosity(>71%). In contrast, for those prepared with higher TDI feeding rate, the specific surface area was significantly reduced together with the pore volume and porosity. To understand these results, it may be necessary to have a briefing on precipitation polymerization. Up to now, this polymerization has been employed mainly as an effective means to fabricate uniform polymer microspheres with neat surface because there is no need for surfactant and stabilizer.[1,2,54,55] The correlative and widely accepted mechanism proposed by Stöver et al.[55] suggests there are two steps in the process with regard to microsphere production: the nucleation of the primitive particles and their growth. At start of the polymerization, the monomers and the solvent form a homogeneous and clear solution. Once the monomers start to polymerize, oligomers are formed. With the polymerization in progress, there is a moment where the oligomers reach their critical length, where they become insoluble in the solvent and start to precipitate out from the solvent and form the primitive particles. The growth of these particles is assumingly accomplished through an "entropy process". Namely, particle growth proceed either through polymerization of oligomers adsorbed on the surface of the primary particles regardless of their length, or through direct polymerization of monomers with reactive groups available on the surface of the same particles. The stability of the particles is assured by the presence of a layer of soluble chain terminals with reactive functional groups chemically bonded to the particle surface. These soluble chain ends tend to extend towards the solvent phase to maximize the entropy of the system, and to protect the particles from collision and aggregation. Their continuous reactions with oligomers or monomers contribute to the particle growth.

Table 1 Porous properties of PPU prepared with different TDI feeding rate (H_2O/acetone ratio 3/7; Total TDI 10 wt%; Stirring rate 300 rpm; Temperature 30 °C)

TDI feeding rate ($mL \cdot h^{-1}$)	Specific surface area ($m^2 \cdot g^{-1}$)	Pore volume ($cm^3 \cdot g^{-1}$)	Porosity (%)
10	163.15	2.11	72.03
20	161.68	2.20	71.77
30	109.39	1.54	65.94
One shot	118.24	1.85	70.43

In the present system, there was no microsphere observed, which indicate that there was no particles formed, or alternatively, primitive particles were formed but immediately aggregated soon after their formation, leading to the porous materials as seen in Fig. 1. From the chemical structure of PPU shown in Scheme 1, one can see that the oligomers (and PPU polymer also of course) are consisting of, alternatively, urea units (-HN-CO-NH-) and methyl-substituted phenylene (-Ph(CH_3)-) units. It is easy to imagine that the chains of PPU oligomers must be highly rigid, and are prone to precipitate out once formed. The primitive particles thus nucleated, hardly to be spherical because of the high rigidity of the chains, most likely do not have the flexible chain ends required to maintain their stability, and a quick aggregation of the particles may take place by consequence. With the polymerization going on, further aggregation between the aggregated primary particles was also to occur, leading to the formation of the porous PPU in large blocks of several dozens of microns, as shown in Fig. 1A. This is quite similar to the phase separation commonly seen in preparation of porous materials,

RSC Advances Accepted Manuscript

which has been often ascribed to the formation of large pores,[24,56,57] and so does the partial aggregation of small particles. This is particularly true with polymers and primary particles of high rigidity, which do not allow them to rearrange their shape, causing the final materials with pore size much larger than that of the interstices if the particles were closely packed.

In summary, it is likely that the polyurea oligomers precipitated out quite soon after their formation to generate small primary particles, which in turn quickly aggregated short of the flexible polymer chains terminals. The polymer chain ends, although not flexible enough to protect the particles from aggregation, were acting, together with the monomer and the oligomers available for surface reaction, as adhesive to stick together the primary particles and the subsequent aggregates, resulting in PPU with large pore. This was in good agreement with the results shown in Fig. 2 (PPU prepared with TDI feeding at 20 mL·h^{-1} and 30 °C), where large pores with diameter between 10 μm and 100 μm were detected.

Fig. 2 shows that the pores with continuous size variation in the tested span from 2 nm to 130 μm were observed. Besides the large pores (size of 10 μm and larger), there were also the pores of small size from 3 nm to 100 nm. Keeping always in mind that the oligomers, the primitive and aggregated particles were of high rigidity, the growth of the particles by further adherence of oligomers under any form onto the interface of PPU-solvent is alike a simple pileup, particularly when PPU surface is rough, because these rigid oligomers lack sufficient conformational flexibility to allow them to rearrange their shape to pack space efficiently. Under this circumstance, there will be solvent trapped between the new pileup and the existing PPU. Evaporation of the trapped solvent molecules will leave nano-and micron-sized pores, similar to the formation of microporous materials by direct synthesis method[57] and to that of the materials of intrinsic microporosity with nano-sized pores,[58-61] where monomers of high rigidity consisting of aromatic rings, like TDI in this work, have been commonly used.

The presence of both large and small pores at the same time in PPU enables one to better understand the results in Table 1, particularly for the two samples with low TDI feeding (10 mL·h^{-1} and 20 mL·h^{-1}). PPU thus prepared was featured by its high specific surface area owing to the presence of small pores in large number, large pore volume and high porosity owing to the presence of abundant large pores. With higher TDI feeding rate (30 mL·h^{-1} or one shot addition), TDI concentration was increased, so was the concentration of amine groups. It is to note that, upon its addition into the reactor, TDI reacted with water first with amine groups immediately formed (Scheme 1). These in-situ formed amines were likely to quickly react with TDI, contributing to the propagation of the oligomer chains and making the oligomers to precipitate out or to be captured by the previously formed particles. At lower TDI concentration (or feeding rate), fresh-added TDI was mostly consumed. With higher TDI feeding rate, it is obvious that the concentration of TDI (and the soluble oligomers) was increased and some of them were trapped inside of the precipitated polymer chains and the porous material (consisting of aggregated primitive particles). And in addition, the molecules of the TDI added at a late stage were also assumed to diffuse into the porous structure if not fully and quickly reacted upon their addition. The polymerization of the TDI molecules present in the inner of the porous material will contribute to reduce the pore size, leaving only the pores of nano-size scaled like those formed in materials of intrinsic microporosity.[58-61] In Fig. 3 are given the pore size distribution of the PPU prepared with TDI feeding rate of 10 mL·h^{-1} and 30 mL·h^{-1}, which demonstrates clearly that, with higher TDI feeding rate, the pores with the size from 2 nm to 500 nm were indeed severely attenuated as expected. Based on this interpretation, the decreases in specific surface area and in pore volume in PPU prepared with TDI feeding of 30 mL·h^{-1} are therefore anticipated. These PPU samples synthesized with different feeding rate were also observed under SEM, which shows that they all possess structure and morphology of typical porous materials (Because of its similarity with Fig. 1, SEM pictures are not given here but in Supporting Information as Fig S1).

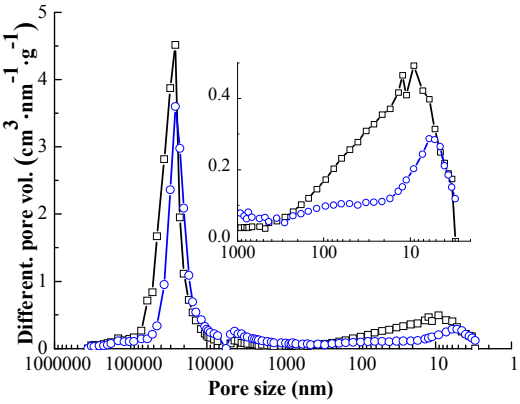

Fig. 3 Pore size distribution and integrated pore volume of PPU prepared with TDI feeding rate of 10 mL·h^{-1} (squares) and 30 mL·h^{-1} (circles)

Porous property and polymerization temperature

To study the influence of polymerization temperature on the porous properties of PPU, a set of polymerization was carried out at varied temperature from 0 °C to 50 °C while keeping the other experimental conditions unchanged (10 wt% of TDI, feeding rate at 20 mL·h^{-1} and H_2O-acetone mass ratio of 3/7 for the solvent). Corresponding results are given in Table 2.

Table 2 Porous properties of PPU prepared at different polymerization temperature (H_2O/acetone ratio 3/7; Total TDI 10 wt%; Stirring rate 300 r·min^{-1}; TDI feeding 20 mL·h^{-1})

Temperature (°C)	Specific Surface area (m^2·g^{-1})	Pore volume (cm^3·g^{-1})	Porosity (%)
0	126.23	1.67	68.42
20	125.21	1.25	61.71
30	161.68	2.20	71.77
50	148.23	3.48	80.33

From Table 2, it is seen that, with polymerization temperature increased from 30 °C to 50 °C, the specific surface area in PPU was decreased with a significant increase in pore volume. From the pore size distribution obtained from Hg intrusion (Because of its similarity to Fig. 2, pore size distribution not given here but in Supporting Information as Fig. S2), it was seen that, in accordance with this increase in temperature, there were obvious increases in the proportion of the large pores (size from 10 μm to

RSC Advances Accepted Manuscript

This journal is © The Royal Society of Chemistry [year]

100 μm) and that of the pores with the size between 20 nm to 1 μm, whereas the extremely small pores (<10 nm) slightly decreased. The increase in the number of the larger pores may be an indication that, with increased polymerization temperature, TDI got polymerized faster, particle nucleation and their subsequent aggregation were promoted, leaving little TDI to fill up the voids formed by the aggregation of the primitive particles. As to PPU prepared at lower temperature (0 °C and 20 °C), an decrease in specific surface combined with decreased pore volume in comparison with that prepared at 30 °C, was detected. Keep in mind that all the runs were conducted with the same TDI feeding rate (20 mL·h^{-1}), the polymerization must be slower at lower temperature, leading to a higher accumulated concentration for TDI and the oligomers. This slow polymerization would give possibility for TDI and the oligomers to diffuse into the pores inside of the porous material, and to get the small pores partially filled up or disappear. Pore size distribution obtained from Hg intrusion demonstrated that there was effectively a substantial decrease in the number of the pores with the size between 10 nm to 1 μm (See Fig. S2 in Supporting Information), in good agreement with the interpretation.

PPU characterization by FTIR

PPU sample and TDI were both subjected to FTIR, the spectra are displayed in Fig. 4. A first observation is that the absorption peak at 2264 cm^{-1}, owing to stretching vibration of NCO, was largely reduced in PPU compared with that in TDI, indicating that TDI was practically all converted to PPU through the described reaction steps (Scheme 1). The strong adsorption peak at 3293 cm^{-1} has been commonly assigned to NH stretching vibration, and the one at 1540 cm^{-1} to NH plane-banding vibration. Note that this vibration of NH were often observed between 1560 cm^{-1} and 1578 cm^{-1},[62,63] it shifted to a lower frequency here owing to the presence of the adjacent aromatic ring and intensive hydrogen-bonding. Urea carbonyl usually has its absorption peaks from 1600 cm^{-1} to 1800 cm^{-1}, depending on its neighboring substituents, and particularly the presence and the extent of hydrogen-bonding and of crystallinity in the materials.[16,64] The peak at 1645 cm^{-1} is assigned to stretching vibration of ordered urea carbonyl. With a urea group attached on phenylene, the vibration absorption of aromatic ring appears usually at 1593 cm^{-1} or 1600 cm^{-1}, so is the peak at 1598 cm^{-1}. Absorption band at 1221 cm^{-1} corresponds to the C-N stretching vibrations.[62] Thus the presence of characteristic groups in the PPU is all confirmed.

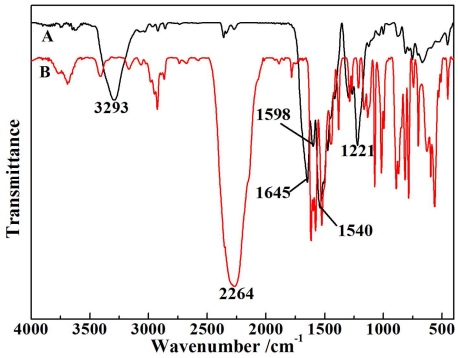

Fig. 4 FTIR spectra of the porous polyurea (A) and TDI (B)

PPU characterization by NMR

It is well known that TDI has a very limited solubility in water, and the reactivity of its two isocyanate groups is quite different.[65,66] It was questionable that polyurea was effectively formed by dispersing TDI in the binary solvent. To this end, PPU as-prepared was undergone ^{13}C and ^{1}H NMR tests. In order to better understand the results, NMR test was also done on 2,4-TDA and TDI monomer (mixture of 2,4- and 2,6-TDI isomers). The spectra of ^{13}C NMR are displayed in Fig. 5. Corresponding chemical shifts are listed in Table 3.

In Table 3, there are two sets of chemical shifts, the ones found in this work (Found) and those calculated (Calcul) based on the additivity principle,[67,68] in which effect of a substituent on chemical shift (δ_{Ci}) of any carbon atom in a given compound is quantized by assign a numerical value (Z_j) as the contribution factor, the chemical shift of a carbon atom in the compound can be theoretically calculated by summing the effects of all substituents by addition of all the contribution factors. Note that, when chemical shift is calculated for different carbon, for a same substituent different value is taken for its contribution factor (Z_j) because its position relative to the carbon on question was changed. Taking 2,4-TDI as an example (chemical structure given in Fig.5), to calculate the chemical shift of any carbon atom i in the phenylene (δ_{Ci}), a base value (128.5 for phenylene) was assigned, and a contribution factor (Z_j) was defined relative to the C_i for each substituent as given in Table 4. This contribution factor for substituent -CH_3 on C_1 is 9.2 (Z_1) when calculating the chemical shift for C_1, those for -NCO on C_2 and C_4 are -3.7 (Z_2) and -2.8 (Z_4); when calculating the chemical shift for C_2, the contribution factor for substituent -CH_3 on C_1 is 0.7 (Z_2) because position C_1 becomes C_2 vis-à-vis C_2; those for -NCO on C_2 and C_4 are 5.1 (Z_1) and 1.1 (Z_3) because position C_2 is now C_1 vis-à-vis C_2, and position C_4 is now C_3 with regard to C_2. For C_1, its calculated chemical shift is therefore: δ_{C1}=128.5+9.2-3.7-2.8=131.2; this calculated chemical shift for C_2 is: δ_{C2}=128.5+0.7+5.1+1.1=135.4. The chemical shift for all the carbon atoms of phenylene was estimated this way, the assignments are listed in Table 3 and accordingly labelled in Fig. 5.

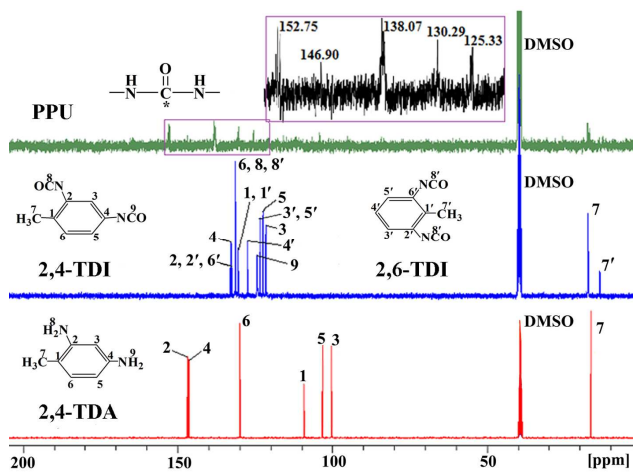

Fig. 5 ^{13}C NMR spectra of 2,4-TDA, TDI and PPU

With all the peaks due to carbon atoms in phenylene assigned, the assignments for the rest of the peaks (C_7 of methyl, C_8 and C_9

RSC Advances Accepted Manuscript

in -NCO groups in Fig. 5) became quite easy. Under the light of reported studies, the peak at 17.30 was assigned to the methyl carbon (C_7), those at 131.30 and 124.20 to the carbons in -NCO attached to carbons 2 and 4 (C_8 and C_9 in Table 3 & Fig. 5), respectively.[21,50,65]

As to PPU spectra, it is to note that all the resonance signals were very weak because of limited solubility of PPU in DMSO. However, with extended scanning time and enlarged spectra (inserted on PPU spectra), one can see quite clearly that, the peaks assigned to the carbon atoms attached to -NCO, seen in TDI spectra (C_2, C_4, $C_{2'}$ and $C_{6'}$, at 132.55 & 132.83), all disappeared. In addition, the characteristic peaks, assigned to -NCO carbons in TDI (C_8, C_9 and $C_{8'}$, at 131.30 & 124.20), were also absent. New peaks around 152.75 appeared, which have been often assigned as characteristic resonance of polyurea.[65,66] These are strong indication that all -NCO (TDI) were effectively reacted.

Table 3 Calculated and experimental chemical shifts on ^{13}C NMR spectra of TDI and 2,4-TDA

C	2,4-TDI δ (ppm)		C	2,6-TDI δ (ppm)		C	2,4-TDA δ (ppm)	
	Calcul.	Found		Calcul.	Found		Calcul.	Found
C_1	131.2	130.44	$C_{1'}$	130.3	130.44	C_1	114.3	109.40
C_2	135.4	132.83	$C_{2'}$,$C_{6'}$	135.4	132.83	C_2	148.2	147.09
C_3	121.0	121.46	$C_{3'}$,$C_{5'}$	121.9	123.29	C_3	101.6	100.58
C_4	131.7	132.55	$C_{4'}$	127.7	127.42	C_4	144.5	146.68
C_5	121.9	122.41	$C_{7'}$	---	13.49	C_5	105.0	103.46
C_6	131.4	131.30	$C_{8'}$	---	131.30	C_6	130.8	130.20
C_7	---	17.30				C_7	---	16.66
C_8	---	131.30						
C_9	---	124.20						

Based on the mechanism of PPU formation (Scheme 1), it is well conceivable that there were primary amines left in PPU. There appeared an obvious peak at 146.9 in ^{13}C NMR spectra of PPU, which is very close to those observed for amine attached carbons in TDA (C_2 & C_4 at 147.09 & 146.68). This suggests that the primary amine (-NH_2) was present in PPU as expected. With -NCO groups turned to urea or -NH_2, their capacity of electron attraction was reduced, which would shift the resonance peaks to a lower field zone for the carbons of phenylene with -NCO attached to before the reaction. The multiple peaks around 138.07 were therefore assigned to the carbons (C_2, C_4, $C_{2'}$ & $C_{6'}$) in PPU.

Table 4 Contribution factor of different substituents on benzene for chemical shift estimation on ^{13}C NMR spectra

Substituents	Value of contribution factor			
	Z_1	Z_2	Z_3	Z_4 [a]
H	0	0	0	0
CH_3	9.2	0.7	-0.1	-3.0
NH_2	18.2	-13.4	0.8	-10.0
NCO	5.1	-3.7	1.1	-2.8

a Obviously, Z_2=Z_6, Z_3=Z_5. Chemical shift δ_{Ci}=128.5+$\sum Z_j$

^{1}H NMR test on PPU was also carried out along with TDI and 2,4-TDA. All the spectra are displayed in Fig. 6. It is easy to distinguish the resonance peaks of the methyl (C_7, $C_{7'}$ in Fig. 6) protons, appeared at 1.90 for TDA and 2.24 for TDI. For PPU, multiple peaks were observed between the chemical shifts 1.90 and 2.24. It is well known that, owing to their electron effect, the substituents on the phenylene have important impact on the chemicals shifts of the protons on phenylene and those in the substituent.[67] With -NH_2, -NCO and a urea unit attached on the aromatic ring as in the present case, this effect pushes the chemical shift of the protons towards lower fields (appearing at higher chemical shift), and the importance of this effect is in the order of -NCO>Urea (-NH-CO-NH-)>-NH_2 in accordance with their capacity as electron acceptor, which implies that the largest chemical shift must occur for the methyl protons in TDI (2.24), the smallest for that in TDA (1.90), and the chemical shift for methyl protons in PPU in between. Because different substitutions, including amine and urea bonds, were possibly present simultaneously in PPU, multiple chemical shifts were therefore observed.

This effect of substituents is equally valid to the chemical shift of the protons of amine attached on benzene in PPU. The chemical shifts of protons in -NH_2, appeared at 4.50 in 2,4-TDA, shifted to 4.80 in PPU (Fig. 6). This assignment of the peak at 4.8 was further confirmed by its vanishing when adding deuterated water (D_2O) in PPU solution in DMSO-d6. The addition of D_2O was to allow the active protons in -NH_2 to be replaced by deuterium, and so that to prove that the peak was effectively originated from -NH_2 in PPU.

When it comes to the resonance signals of the protons directly attached on phynelene, the same effects, as that discussed on chemical shifts of -NH_2 protons imposed by the substituents, were well observed. Chemical shifts of the protons on carbons 3, 5 & 6 in TDA appeared at 5.77, 5.89 and 6.56, those in TDI at 7.01, 7.40 & 7.18. More than three peaks were seen in TDI because TDI used here is a mixture of 2,4 and 2,6 substituted isomers. As to PPU, the resonance became more complicated with the use of TDI isomers, because the isocyanate group in the final polyurea may be present as a urea unit (-NH-CO-NH-, main repeating unit in PPU), as amine (when reacted with H_2O only as in the case where no more TDI available at end of the polymerization, or where the amine ended oligomers wrapped up in the precipitation polymerization), and even as residual -NCO groups in small amount. Note that the protons in urea unit in PPU (-NH-CO-NH-) should also have their chemical shifts between 6.5 and 10.0.[50,69,70] With all these combined, the chemical shifts were observed in a wide span from 6.20 to about 9.0 as seen in Fig. 6.

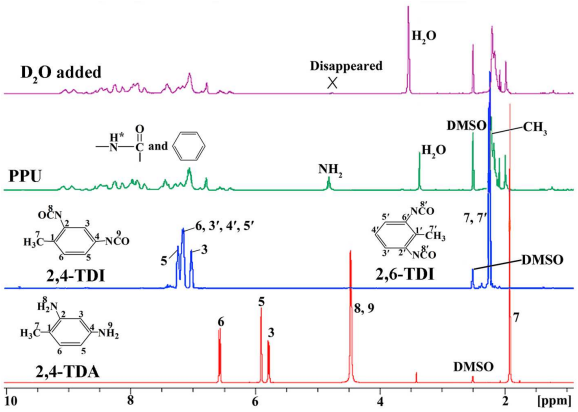

Fig. 6 ^{1}H NMR spectra of 2,4-TDA, TDI and PPU

It is conceivable that, for a polyurea chain, there are two

This journal is © The Royal Society of Chemistry [year]

RSC Advances Accepted Manuscript

terminal -NH_2 groups upon polymerization. The intensity of the peak at 4.80, belonging to the protons of -NH_2, was quite obvious. This is an indication that the degree of polymerization of PPU may be very low. To clarify this point, the polymerization degree of PPU was estimated by comparing the integrated area of the resonance peaks at 4.80 with that owing to the protons of the methyl on phenylene in PPU, present between 1.93 and 2.20. Assuming the degree of polymerization (or the number of phenylene in PPU) being X (the number of TDI units, equal also to the number of methyl group), the proton number in methyl is 3X in one polyurea chain, and that in terminal -NH_2 is always 4, because PPU here is linear polyurea (the hydrogen in urea unit is not active enough under present experimental condition[49,50]). The peak area for methyl protons was determined to be 11.23, and that of -NH_2 was 0.99. The following equation was established:

$$\frac{Number\ of\ CH_3\ protons}{Number\ of\ NH_2\ protons} = \frac{3X}{4} = \frac{11.23}{0.99}$$

From this equation, X=15 was obtained. This indicates that this PPU material was in fact consisting of short polymer chains with degree of polymerization of about 15.

Crystallization characteristics

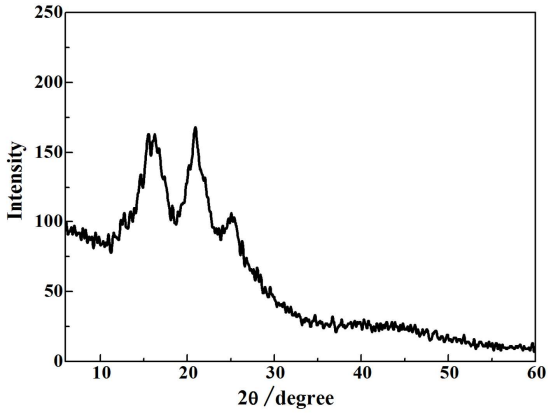

Fig. 7 XRD diffractogram of PPU

The presence of ordered structure and crystallinity in polyureas has been often suggested.[14,16,18,64,71] FTIR analysis seems also supportive to this point. To have a further confirmation to the presence of crystallinity in PPU, it was subjected to XRD test. The diffractogram is given in Fig. 7, from which one can see clearly three diffraction peaks with 2θ at 16.11º, 20.92º and 25.11º. Through Bragg equation, one can easily figure out that these 2θ values correspond to interplanar spaces of 5.497 Å, 4.243 Å and 3.544 Å, respectively. It has been recognized that, the presence of hydrogen-bonding due to the polar carbonyl and amide group in urea units, combined with the rigidity of the backbone with abundant benzene rings, leads often to ordered structure, even crystallinity between two neighboring polymer chains. There were also studies,[16,18] which concluded that one carbonyl in a polyurea chain could associate with two -NH- in the neighboring polymer chain, leading to the hydrogen-bonding with a interplanar space of 4.243 Å, between two phenylene rings in two different polyurea chains, as depicted in Fig. 8A.[71] As to the diffraction peak at 16.11º, it was believed to be due to the formation of the hydrogen-bonding between a carbonyl in a polyurea chain and a phenmethyl unit in the neighboring polymer chain, leading to the interplanar space of 5.497 Å between two phynelene rings as shown in Fig. 8B.[14,16,18,71] These XRD data provide therefore a reliable confirmation that there was indeed presence of crystallinity in this PPU material

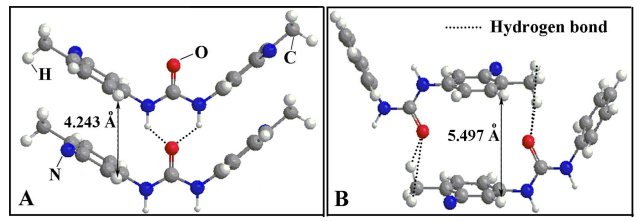

Fig. 8 Possible chain conformations owing to urea-urea (A) and urea-methyl interaction (B) in polyurea (gray, white, red and blue spheres stand for C, H, O and N atoms respectively)

Thermal properties of PPU

By XRD analysis, it seems that there may exist highly ordered structure or crystallinity in PPU owing to the abundant presence of hydrogen-bonding in similar polyurea and polyurethane materials.[16,64] To have a better understanding, DSC test on PPU was carried out along with TGA and DTA (Fig. 9). On the DSC curve, it seems that a likely fusion peak related to crystal melting appears at 332 °C, DTA test indicated also a crystal fusion at 333°C (not show here), practically at the same temperature. In fact, this high melting points have been also reported, for a polyurea at 370 °C,[16] and for another polyurea based on 4,4'-diphenylmethane diisocyanate at 346 °C.[15] However, when conducting TGA test, it was seen that PPU started to have an appreciable weight loss (5%) at about 275 °C, it lost 50% of its initial mass at 322 °C. And at 336 °C, 90% of the sample was degraded. This indicates that the fusion temperature at 332°C detected by DSC completely superposed with the decomposition of PPU. A full examination of the fusion process was impossible.

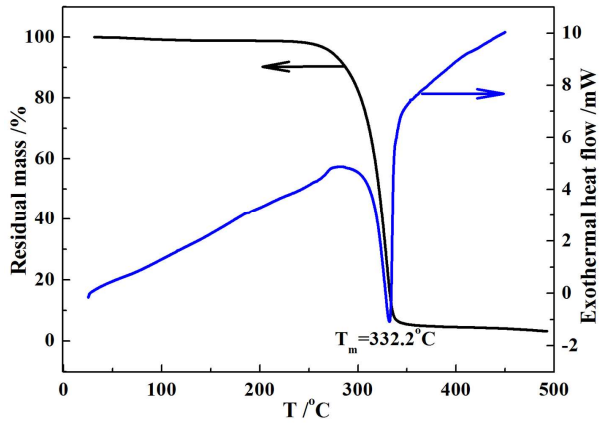

Fig. 9 DSC and TGA curves of the PPU

Conclusions

Porous polyurea (PPU) is prepared through a simple protocol of precipitation polymerization of TDI at 30 °C. The polymerization starts with TDI reaction with water to yield diamine in a binary solvent of water-acetone at mass ratio of 3/7 (H_2O/acetone), followed by step polymerization of the in-situ produced diamine

RSC Advances Accepted Manuscript

with TDI. PPU as-prepared has a specific surface area of 161.68 $m^2 \cdot g^{-1}$, a porosity of 71.77% and a pore volume of 2.20 $cm^3 \cdot g^{-1}$. Pores with size varying from 2 nm to 130 μm are present, with the pore size mainly presented between 10 μm and 40 μm. PPU is analyzed by FTIR and NMR (^1H & ^{13}C), the presence of characteristic groups in the PPU is all confirmed. These analyses show that TDI is full reacted and polyurea was effectively obtained. NMR tests confirm also that PPU is consisting of short polyurea chains with degree of polymerization of about 15. The presence of crystallinity in PPU is further confirmed by X-ray diffraction, which shows three diffraction peaks. Through Bragg equation, corresponding interplanar spaces owing to different hydrogen-bonding and associated polymer chain conformation are depicted. TGA analysis demonstrates that PPU is of high thermal stability, and no degradation is seen before 270 °C. DSC test reveals that no obvious glass transition is observed owing to intensive hydrogen-bonding. The fusion temperature of the crystal structures fully coincides with PPU decomposition, which makes the observation of the fusion process difficult by DSC.

Acknowledgements

This research is financially supported by Natural Science Foundation of China (NSFC, No. 21274054, 21304038) and by Science & Technology Development Plans of Shandong Province, China (No. 2010GSF10610).

Notes and references

[a] *College of Chemistry and Chemical Engineering, University of Jinan, Jinan, China, 250022; E-mail: xzkong@ujn.edu.cn;*
[b] *College of chemistry and Chemical Engineering, Shandong University, Jinan, China, 250100*

† Electronic Supplementary Information (ESI) available: [SEM pictures of PPU prepared with different TDI feeding rate in H_2O-acetone with H_2O/acetone mass ratio at 3/7 and 10 wt% of TDI concentration; Pore size and size distribution of the PPU prepared at different polymerization temperature (0 °C; 20 °C; 30 °C; 50 °C)]. See DOI: 10.1039/b000000x/

1 X. Jiang, X. Z. Kong and X. Zhu. *J. Polym. Sci. Part A* 2011, **49**, 4492-4497.
2 X. Jiang, X. Zhu and X. Z. Kong. *Chem. Eng. J.* 2012, **213**, 214-217.
3 S. Li, X. Z. Kong, X. Jiang and X. Zhu. *Chinese Chem. Lett*. 2013, **24**, 287-290.
4 W. H. Awad, C. Nyambo, S. Kim, R. J. Dinan, J. W. Fisher and C. A. Wilkie, in *Fire and Polymers V. ACS Symposium Series, Vol. 1013*. Eds. C. A. Wilkie1, A. B. Morgan. and G. L. Nelson. Am. Chem. Society. Washington DC, 2009, pp. 102-117.
5 J. S. Davidson, J. W. Fisher, M. I. Hammons, J. R. Porter and R. J. Dinan. *J. Struct. Eng.* 2005, **131**, 1194-1205.
6 M. S. Hoo-Fat, X. Ouyang and R. J. Dinan. *Mater. Struct*. 2004, **15**, 129-38.
7 D. Mohotti, T. Ngo, P. Mendis and S. N. Raman. *Mater. Design.* 2013, **52**, 1-16.
8 K. Ackland, C. Anderson and T. D. Ngo. *Int. J. Impact Eng.* 2013, **51**, 13-22.
9 A. Samiee, A. V. Amirkhizi and S. Nemat-Naser. *Mech. Mater.* 2013, **64**, 1-10.
10 D. Koyama and K. Nakamura. *Appl. Acoust.* 2010, **71**, 439-445.
11 P. Cass, W. Knower, T. Hinton, S. Shi, F. Grusche, M. Tizard and P. Gunatillake. *Acta Biomater.* 2013, **9**, 8299-8307.
12 S. V. Ley, C. Ramarao, A. L. Lee, N. Østergaard, S. C. Smith and L. M. Shirley. *Org. Lett.* 2003, **5**, 185-187.
13 G. D. Yadav and Y. S. Lawate. *Ind. Eng. Chem. Res.* 2013, **52**, 4027-4039.
14 S. K. Yadav, K. C. Khilar and A. K. Suresh. *J. Membr. Sci.* 1997, **125**, 213-218.
15 H. Ishihara, I. Kimura and N. Yoshihara. *J. Macromol. Sci. Phys.* 1983-84, **B22**, 713-733.
16 N. Luo, D. N. Wang and S. K. Ying. *Polymer* 1996, **37**, 3577-3583.
17 L. Zhu, C. Y. Huang, Y. H. Patel, J. Wu and S. V. Malhotra. *Maromol. Rapid Commun.* 2006, **27**, 1306-1311.
18 L. Q. Feng and J. O. Iroh. *Eur. Polym. J.* 2013, **49**, 1811-1822.
19 M. Kim, M. Byeon, J. S. Bae, S. Y. Moon, G. Yu, K. Shin, F Basarir, T. H. Yoon and J. W. Park. *Macromolecules* 2011, **44**, 7092-7095.
20 S. Y. Moon, J. S. Bae, E. Jeon and J. W. Park. *Angew. Chem. Int. Ed.* 2010, **49**, 9504-9508.
21 N. Leventis, C. Sotiriou-Leventis, N. Chandrasekaran, S. Mulik, Z. J. Larimore, H. Lu, G. Churu and J. T. Mang. *Chem. Mater.* 2010, **22**, 6692-6710.
22 L. Weigold, D. P. Mohite, S. Mahadik-Khanolkar, N. Leventis and G. Reichenauer. *J. Non-Cryst. Solids* 2013, **368**, 105-111.
23 B. Cheng, Y. Le, W. Cai and J. Yu, *J. Hazard. Mater.* 2011, **185**, 889-897.
24 M. T. Gokmen and F. E. Du Prez. *Prog. Polym. Sci.* 2012,**37**, 365-405.
25 M. S. Silverstein. Polymer 2014, **55**, 304-320.
26 G. L. Li, H. Möhwalda and D. G. Shchukin. Chem..Soc..Rev. 2013, **42**, 3628-3646.
27 P. Monvisade and P. Siriphannon, *Appl. Clay Sci*. 2009, **42**, 427-431.
28 H. Schönfeld, K. Hunger, R. Cecilia and U. Kunz, *Chem. Eng. J.* 2004, 101, 455-463.
29 J. Liu, J. Yao, H. Wang and K. Chan, *Green Chem.* 2006, **8**, 386-389.
30 S. Samatya, E. Orhan, N. Kabay and A. Tuncel, *Colloid Surface A* 2010, **372**, 102-106.
31 M. Slater, M. Snauko, F. Svec and M. J. Fréchet, *Anal. Chem.* 2006, **78**, 4969-4975.L. Han, H. J.
32 F. Barahona, E. Turiel and A. Martín-Esteban, *J. Chromatogr. A* 2011, **1218**, 7065-7070.
33 L. Han, H. J. Choi, D. K. Kim, S. W. Park, B. Liu and D. W. Park, *J. Mol. Catal.* A 2011, **338**, 58-64.
34 K. M. Thomas, *Catal. Today* 2007, **120**, 389-398.
35 H. Kawakita, K. Sugita, K. Saito, M. Tamada, T. Sugo and H. Kawamoto, *J. Membr. Sci.* 2002, **205**, 175-182.
36 M. Gulfam, J. M. Lee, J. Kim, D. W. Lim, E. K. Lee and B. G. Chung, *Langmuir* 2011, **27**, 10993-10999.
37 Q. Zhang, L. V. Saraf, J. R. Smith, P. Jha and F. Hua, *Sensor Actuat.* A 2009, **151**, 154-158.
38 M. G. Rabbani and H. M. El-Kaderi, *Chem. Mater*. 2011, **23**, 1650-1653.
39 R. Liu, P. Liao, J. Liu and P. Feng, *Langmuir* 2011, **27**, 3095-3099.
40 A. B. Moustafa, T. Kahil and A. Faizalla, *J. Appl. Polym. Sci.* 2000, **76**, 594-601.
41 J. Xu, G. Chen, R. Yan, D. Wang, M. Zhang, W. Zhang and P. Sun, *Macromolecules* 2011, **44**, 3730-3738.
42 J. W. Kim and K. D. Suh, *J. Ind. Eng. Chem.* 2008, **14**, 1-9.
43 R. A. Prasath, M. T. Gokmen, P. Espeel and F. E. Du Prez, *Polym. Chem.* 2010, **1**, 685-692.
44 X. Li, X. Wang, G. Ye, W. Xia and X. Wang, *Polymer* 2010, **51**, 860-867.
45 L. Yang, Y. Li, X. Jin, Z. Ye, X. Ma, L. Wang and Y. Liu, *Chem. Eng. J.* 2011, **168**, 115-124.
46 M. A. L. Tanco, D. A. P. Tanaka, V. C. Flores, T. Nagase and T. M. Suzuki, *React. Funct. Polym.* 2002, **53**, 91-101.
47 M. V. Dinu and E. S. Dragan, *React. Funct. Polym.* 2008, **68**, 1346-1354.
48 H. A. Patel and C. T. Yavuz, *Chem. Comm.* 2012, **48**, 9989-9991.
49 Z. Li, T. Zhang, S. Niu and C. Xu. *Spectrosc. Soect. Anal.* 2003, **23**, 1107-1110.
50 A. Lapprand, F. Boisson, F. Delolme, F. Méchin and J. P. Pascault. *Polym. Degrad. Stab.* 2005, **90**, 363-373.
51 G. H. Zhang, R. X. Hou, D. X. Zhan, Y. Cong, Y. J. Cheng and J. Fu. *Chinese Chem. Lett*. 2013, **24**, 710-714.
52 H. O. Song, Y. Zhou, A. M. Li and S. Mueller. *Chinese Chem. Lett*. 2012, **23**, 603-606.
53 B. Pan, B. Pan, W. Zhang, L. Lü, Q. Zhang and S. Zheng. *Chem. Eng. J.* 2009, **151**, 19-29.

RSC Advances Accepted Manuscript

This journal is © The Royal Society of Chemistry [year]

54 X. Z. Kong, X. Gu, X. Zhu and L. Zhang, *Macromol. Rapid Comm.* 2009, **30**, 909-914.
55 J. S. Downey, R. S. Frank, W. H. Li and H. D. H. Stöver. *Macromolecules* 1999, 32, 2838-2844.
56 J. Fan, C. Yu, B. Tu and D. Y. Zhao, *Chem. J. Chinese Univ*. 2001, 22, 1459-1461.
57 D. Wu, F. Xu, B. Sun, R. Fu, H. He and K. Matyjaszewski. *Chem. Rev.* 2012, 112, 3959-4015.
58 N. B. McKeown and P. M. Budd, *Macromolecules* **2010**, *43*, 5163-5176.
59 J. Germain, J. M. J. Fréchet and F. Svec, *Chem. Comm.* **2009**, *(12)*, 1526-1528.
60 C. M. A. Parlett, K. Wilson and A. F. Lee, *Chem. Soc. Rev.* **2013**, *42*, 3876-3893.
61 G. Cheng, T. Hasell, A. Trewin, D. J. Adams and A. I. Cooper, *Angew. Chem. Int. Ed.* **2012**, *51*, 12727-12731.
62 C. Zhong, D. Chen, Y. Zhang and B. Hou. *Speciality Petrochem.* 2007, **24**, 67-70.
63 N. Ketata, C. Sanglar, H. Waton, S. Alamercery, F. Delolme, O. Paisse, G. Raffin and M. F. Grenier-Loustalot. *Polym. Polym. Comp*. 2004, **12**, 645-665.
64 N. Luo, D. N. Wang and S. K. Ying. *Polymer* 1996, **37**, 3045-3047.
65 T. Gebauer, A. T. Neffe and A. Lendlein. *MRS Proceedings*, 1569, mrss 10-17, 2013. Doi:10.1557/opl.2013.839.
66 D. C. Allport, D. S. Gilbert and S. M. Outterside. *MDI and TDI: Safety, Health and the Environment: A Source Book and Practical guide.* John Wiley & Sons, Ltd. Chickester, UK, 2003, pp. 237-238.
67 E. Pretsch, P. Biihlmann and C. Affolter. *Structure Determination of Organic Compounds-Tables of Spectral Data.* Springer-Verlag, Berlin & Heidelberg, 3rd Edn, 2000, pp. 96-98.
68 P. E. Hansen. *Org. Magn. Reson.* 1979, **12**, 109-142.
69 M. Sumi, Y. Chokki, Y. Nakai, M. Nakabayashi and T. Kanzawa. *Makromol. Chem.* 1964, **78**, 146-156.
70 H. Okuto. *Die Makromol. Chem.* 1966, **98**, 148-163.
71 L. Born and H. Hespe. *Colloid Polym. Sci*. 1985, **263**, 335-376.

RSC Advances Accepted Manuscript

Graphic Abstract

One step preparation of porous polyurea by reaction of toluene diisocyanate with water and its haracterization

Hui Han[a], Shusheng Li[a,b], Xiaoli Zhu[a], Xubao Jiang[a] and Xiang Zheng Kong*[a]
a. College of chemistry and Chemical Engineering, University of Jinan, Jinan, China, 250022
b. College of chemistry and Chemical Engineering, Shandong University, Jinan, China, 250100

Porous polyurea is synthesized by reacting toluene diisocyanate with water in water-acetone binary solvent. Material characterizations lead to likely conformations of the polymer chains owing to presence of intensive H-bonding.

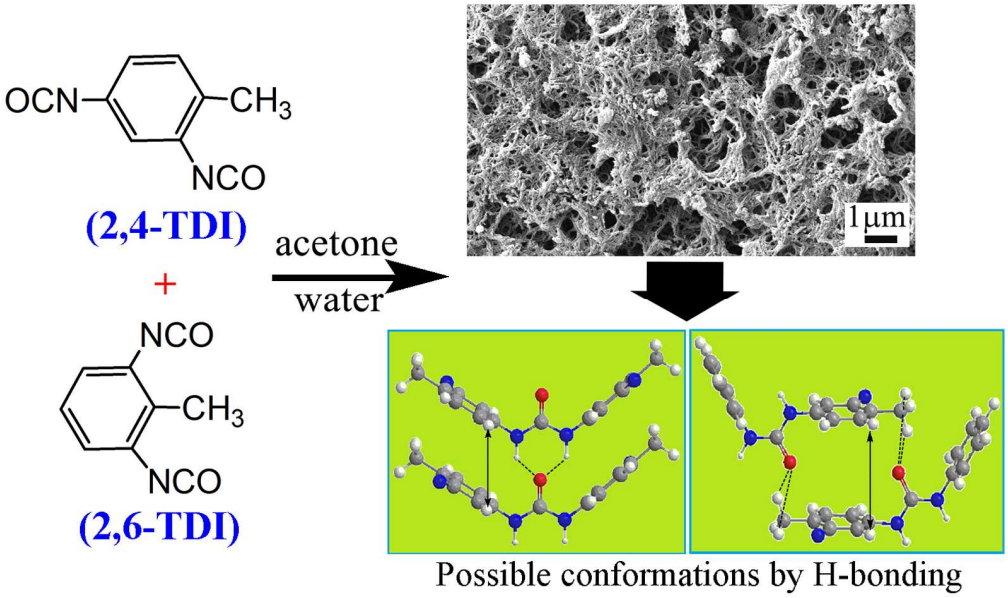

RSC Advances Accepted Manuscript